



Article

Damping Characteristics of Viscoelastic Damping Structure under Coupled Condition

Jun Wang, Dagang Sun *, Shizhong Liu and Xin Zhang

College of Mechanical Engineering, Taiyuan University of Science and Technology, Taiyuan 030024, China; wj3201239@163.com (J.W.); liusz2000@163.com (S.L.); zhangxinbox@126.com (X.Z.)

* Correspondence: sundgbox@sina.com; Tel.: +86-351-6998115

Academic Editor: Fazal M. Mahomed

Received: 18 November 2016; Accepted: 3 March 2017; Published: 15 March 2017

Abstract: Temperature has an influence on damping characteristics of the viscoelastic damping structure. The change of the damping characteristics of the structure under the cycle load is a dynamic and coupled process. The hyperelastic-viscoelastic model was used to describe nonlinear deformation and viscoelasticity simultaneously. The temperature distribution and change of the damping characteristics under the coupled condition was analyzed by finite element method (FEM). The maximum value of the simulation results was in agreement with the one calculated by the formula in the literature. Dynamic stiffness and dissipated energy were obtained based on the hysteresis loop. Dynamic stiffness and dissipated energy gradually decreased with the increase of the temperature.

Keywords: viscoelastic damping structure; hyper-viscoelasticity; damping characteristics; thermal-mechanical coupling

1. Introduction

The viscoelastic damping structure is widely applying for vibration and noise reduction. The viscoelastic damping layer, most of which is rubber or rubberlike polymers, represents hysteresis under a dynamic load. Part of the mechanical energy is absorbed and finally dissipated as heat due to the internal friction of the molecular chains. Continuous cyclic load and poor conduction of heat may cause extensive heat to build up in the structure. The mechanical response of the viscoelastic materials is often highly sensitive to temperature [1–3]. Heat may change the mechanical characteristics of the structure and the damping capability [4–6]. Excessive heat may lead to early fatigue failure or even explosive rupture. Therefore, it is essential to evaluate the temperature distribution and damping characteristics of the viscoelastic damping structure due to the mechanical energy dissipation during cyclic loading.

Numerous analyses have been proposed to estimate the temperature distribution and damping characteristics of viscoelastic material and its structure. Macro-mechanical or micro-mechanical material models were proposed to describe thermo-viscoelastic behavior [7–10]. The complexity of the theory restricts their engineering application. Habibi et al. investigated structural bamboo at the microscopic and macroscopic level [11]. Two kinds of biological cells separately have the responsibility of viscoelasticity at lower or higher frequencies. David I. G. Jones introduced simple and effective approaches for describing the damping-related properties of viscoelastic materials, with emphasis on the effects of frequency and temperature, and proceeded to illustrate simple techniques for measuring the desired properties and for selecting and applying the materials [12]. Johnson and Chen employed a linear viscoelastic model (the Maxwell solid model) to solve the coupled thermal and large strain history integral. Due to under-prediction of the size of the hysteresis loop in the linear viscoelasticity, the error in dissipated energy prediction at large strain is unacceptable [13].

Shah et al. studied the coupled problem of deformation of a linear-viscoelastic composite cylinder by applying the correspondence principle [14]. Pesek et al. proposed a mathematical model based on a weak formulation of the partial differential equation by FEMLAB (original release of COMSOL Multiphysics) to investigate the thermo-mechanical interaction in a pre-stressed rubber block used for resilient elements of composed tram wheels. A proportional damping model and the equality of the heat energy density and the dissipation energy density were computed to perform coupling between the mechanical and thermal equations under selected simple stress states [15]. Banic et al. investigated the temperature of a rubber damper under cyclic loading due to hysteresis losses by finite element analysis (FEA). The visco-plastic constitutive model established by Bergstrom-Boyce was used to predict the heat generation and hysteresis in the rubber-metal spring of railway draw gear [16]. Luo et al. predicted the heat generation of a rubber spring instrument during the spring-accelerated fatigue test. A static hysteresis loop was obtained via the FEA approach experimentally [17]. Kamran and Anastasia used a non-linear visco-elastic constitutive model (proposed by Schapery) to analyze the effect of coupling between the thermal and mechanical response, which was attributed to the dissipation of energy, heat conduction and temperature-dependent material parameters on the overall response of visco-elastic solids [18]. Hwang and Yeong analyzed the temperature distribution of a coupled 3D dynamic rolling simulation of a tire by finite element method (FEM) [19]. The heat generation rate was assumed to be equal to the strain energy density function multiplied by the hysteresis coefficient. Fenza et al. investigated the damping characteristics of a viscoelastic embedded composite fuselage structure by experiments at different temperatures [20]. Kerchman and Cheng [21] evaluated the heat generation and transient temperature using linearized constitutive model and FEM. Frequency-dependence on the Viscoelastic Damping VED structure is also a matter of major concern. The sandwich viscoelastic damping structure is analyzed by the method of model reduction to reduce the high-order finite element models to a smaller size in direct dynamic analysis [22]. The frequency response analysis of viscoelastic beams and plane frames with an arbitrary number of Kelvin-Voigt viscoelastic dampers was concerned. The exact frequency response in all frame members was also obtained in closed analytical form [23].

Since the damping characteristics of viscoelastic material are sensitive to temperature, also due to the low conductivity of the material, the damping ability is a dynamic coupled process. Some works treated the coupled problem with a one-way coupling approach, especially common in the rolling resistance field of rubber tires. Some coupled thermo-mechanical constitutive models need to user-defined material (UMAT) subroutine by support. Meanwhile, due to the coupled effect, the temperature distribution of the viscoelastic damping structure may not be constant or homogeneous. In this paper, a fully coupled analysis of the viscoelastic damping structure will be investigated to describe the change of the damping characteristics more accurately. The investigation by commercial finite code ABAQUS (Dassault Systèmes, Vélizy-Villacoublay, France) will be validated by comparing it with the available field data in the present literature.

2. Simulation Method

2.1. Hyper-Viscoelastic Model

Viscoelastic materials usually represent large deformation and dynamic characteristics simultaneously. The linear viscoelastic models do a poor job of replicating the hysteresis loop in a load/unload cycle of deformation because the hysteresis loops generated are narrow. Therefore, the combined usage of the hyperelasticity and linear viscoelasticity (usually described as a Prony series) is used for the hysteresis analysis. The stress response of the hyper-viscoelastic model consists of a nonlinear elastic part and a viscous part. The elastic response is instantaneous while the viscous part is prolonged over time. More details of the constitutive model as formulations and implementation are available in the literature [24,25]. The hyperelastic response (time-independent) is generally derived from stress-strain data by tensile, compression, shear and/or biaxial tests. There stress-strain

data may be fitted as a particular strain energy function by the linear or nonlinear least squares method. The dynamic mechanical characteristics may be obtained by the dynamic mechanical analyzer (DMA). The Prony series parameters were fitted by the optimization method. For simplicity, the constitutive parameters of the material were from the example in the ABAQUS Example Problem Manual article [26,27]. All units of British thermal units (BTU) parameters were translated into the international system of units (SI).

The hyperelastic response is described as the Neo Hooke model:

$$U = C_{10}(\bar{I}_1 - 3) + \frac{1}{D_1}(J_{el} - 1)^2 \quad (1)$$

where C_{10} is the positive material parameter, $C_{10} = 1.0423 \times 10^3$, psi = 7.1864×10^6 Pa, and D_1 controls compressibility, $D_1 = 9.6267 \times 10^{-6}$.

The N-term Prony series:

$$g(t) = g_{\infty} + \sum_{i=1}^N g_i \exp(-t/\tau_i) \quad (2)$$

where g_{∞} and g_i are normalize dimensionless constants and $g_{\infty} + \sum_{i=1}^N g_i = 1$.

The Prony parameters were as follows: $g_1 = 0.0396$, $t_1 = 1.766$. $g_2 = 0.1018$, $t_2 = 0.1536$. $g_3 = 0.858$, $t_3 = 0.0127$.

2.2. Finite Element Method (FEM) Implementation

For temperature dependence, most viscoelastic materials are usually assumed as thermal rheological simple (TRS) material near or above the glass transition temperature. The TRS translation function is expressed by the Williams–Landel–Ferry (WLF) equation [28]:

$$\log A = -\frac{C_1(\theta - \theta_0)}{C_2 + (\theta - \theta_0)} \quad (3)$$

where the values are defined as $\theta_0 = 21.7$ °C, $C_1^0 = 56.1$ °C, and $C_2^0 = 1000$ °C.

By means of the backward difference method, the temperature is integrated into the Newton method for solving nonlinear equations. Its exact solution algorithm [28]:

$$\begin{bmatrix} K_{uu} & K_{u\theta} \\ K_{\theta u} & K_{\theta\theta} \end{bmatrix} \begin{Bmatrix} \Delta u \\ \Delta \theta \end{Bmatrix} = \begin{Bmatrix} R_u \\ R_{\theta} \end{Bmatrix} \quad (4)$$

where Δu and $\Delta \theta$ are the respective corrections to the incremental displacement and temperature, K_{ij} are sub-matrices of the fully coupled Jacobian matrix, R_u and R_{θ} are the mechanical and thermal residual vectors, respectively.

A viscoelastic damping structure consisting of two elastic constrained layers and one viscoelastic damping layer was accomplished by the solution of temperature displacement in ABAQUS. The length was 0.09 m with 45 elements. The thickness of the elastic constrained layer and the viscoelastic damping layer was 0.01 m with eight elements. The elastic constrained layer was discretized into 4-node plane strain thermally coupled quadrilateral (CPE4T) elements and 4-node plane strain thermally coupled quadrilateral (CPE4HT) elements for the viscoelastic damping layer. A sinusoidal displacement $U = 0.0064 \sin \omega t$ ($\omega = 2\pi f$, $f = 1$ Hz) in the x direction was applied on the top left-hand corner. The bottom side was completely fixed (Figure 1). Heat generation by hysteresis is associated with intrinsic dissipation due to plasticity, which is usually described by inelastic heat friction (IHF). IHF is defined by the ratio of the dissipated energy to the plastic work [29]. For viscoelastic materials, the IHF is assumed to be 1.071×10^{-4} in the ABAQUS help documentation. The properties of materials

refer to the ABAQUS Example Problem Manual article (Table 1). The initial temperature was 21.7 °C. An adaptive time stepping was determined with a creep strain error tolerance of 5×10^{-3} .

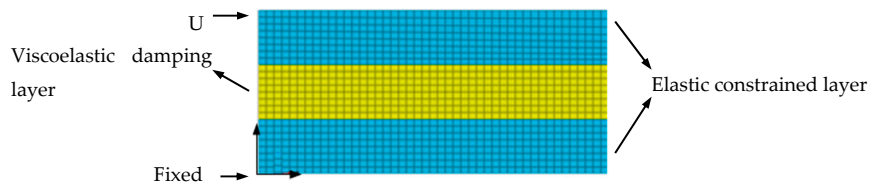


Figure 1. Finite Element (FE) model of viscoelastic structure.

Table 1. Properties of materials.

Property	Elastic Constrained Layer	Viscoelastic Damping Layer
Density (kg/m ³)	7850	1130
Modulus of elasticity (Pa)	2.1×10^{11}	-
Poisson ratio	0.3	-
Thermal expansion coefficient (10 ⁻⁶ (m/m.K))	10.8	220
Specific heat capacity (J/kg.°C)	502	1900
Heat conduction (W/(m.°C))	70	0.14
Non-elastic thermal friction coefficient	-	1.071×10^{-4}

3. Results and Discussion

3.1. Temperature Distribution

The temperature distribution in the end was contoured on a postprocessor (Figure 2). The temperature adjacent to the elastic constrained layer nearly maintained the ambient temperature (21.7 °C) due to pure elasticity and excellent thermal conductivity. The temperature was increased from the outside to the inside as concentric circle in the viscoelastic damping layer. The maximal value θ_{\max} appeared in the center, and reached 28.1 °C. The same result could be found in the ABAQUS Example Problem Manual article.

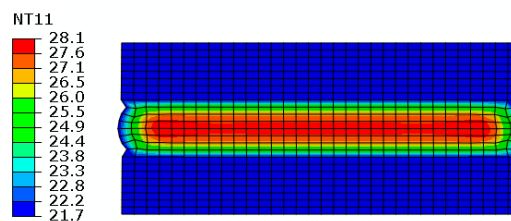


Figure 2. Temperature (°C) contour in the end.

The value for θ_{\max} can also be calculated by the next formula [30]:

$$\theta_{\max} = \theta + \frac{fU_d H^2}{8K} \tag{5}$$

where θ is the initial temperature, f is the frequency of the loading cycles, H is the thickness of the viscoelastic component, K is the heat conduction of the viscoelastic material, and U_d is the amount of energy generated per cycle:

$$U_d = \pi E_2 \varepsilon_0^2 \tag{6}$$

where E_2 is the loss modulus of the viscoelastic material and ε_0 is the amplitude of the strain.

Further, θ_{\max} calculated at 28.9 °C by Equation (5) matched well with the simulation (28.1 °C). The simulation error was 2.7%, so it is clear that the proposed method has the advantages of high accuracy to evaluate the maximal value of the temperature distribution.

3.2. Dynamic Damping Characteristics

In this part, the change of the dissipated energy and dynamic stiffness were discussed. The hysteresis loop is generated by load and displacement due to hysteresis behavior. The integration area of the hysteresis loop is the dissipated energy E_d , which represents the ability of the viscoelastic damping structure. The reaction force of every node RF_n on the bottom and displacement x of left corner on the top were extracted separately on the postprocessor. The reaction force of the structure RF was summed by RF_n . The combined RF with x the hysteresis curve was drawn (Figure 3a). The hysteresis loop did not form completely in the first period, so E_d was calculated from the second period to the end. E_d was reduced with the increase of the temperature. With the temperature increased, the relaxation time of the intermolecular motion was shortened. The dissipated energy was decreasing because the motion of the molecule gradually kept up with the external force [13]. Dynamic stiffness is defined as GB/T 15168-2013 [31]

$$F_d = \frac{F_0}{X_0} \cdot \frac{y'}{x'} \tag{7}$$

where F_0 is double amplitude in maximal displacement, X_0 is double amplitude corresponding to the transmitting force, x' is the displacement per unit length on the x-axis, and y' is the force per unit length on the y-axis (Figure 3b). Thirty percent of the dynamic stiffness was decreased in the period of loading. A similar result was found by Liu [23]. Both the stiffness and damping coefficient decreased with the temperature increasing. Creep was aggravated by the temperature rising while the carrying capacity of the viscoelastic damping structure decreased. With the increase of the total number of cycles, the elastic modulus or stiffness of the material decreases. It is a common phenomenon that the structural stiffness cannot bear external load before the material has been destroyed. The ability of the dissipated energy will strongly decline. The change of E_d and F_d were seen in Figure 4.

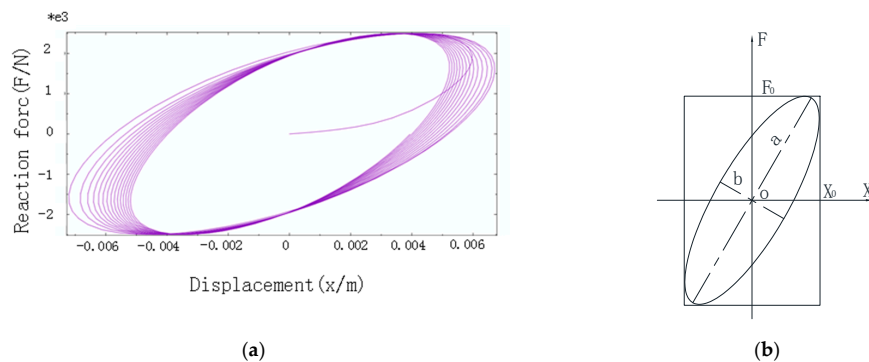


Figure 3. Hysteresis loops (a) Coupled hysteresis loop; (b) Schematic diagram.

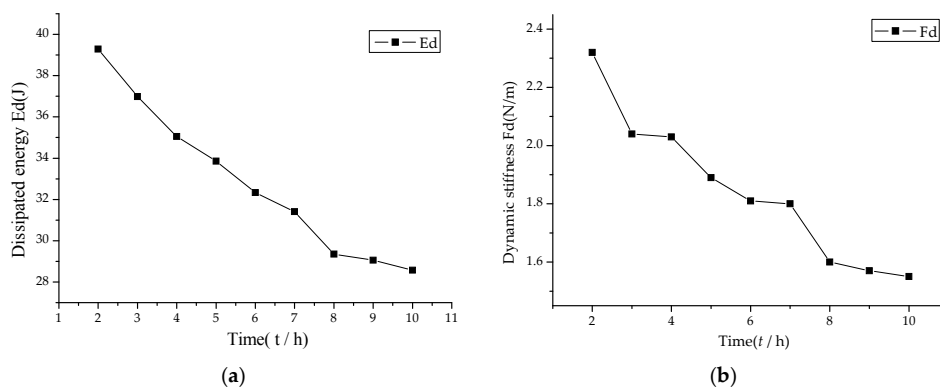


Figure 4. Change of dynamic damping characteristics. (a) Dissipated energy (E_d); (b) Dynamic stiffness (F_d).

4. Conclusions

The aim of this research was to investigate the temperature distribution and change of the damping characteristics of the viscoelastic damping structure under a coupled condition. A hyper-viscoelastic constitutive model was employed to describe the hyperelastic response and viscoelastic response. A two-dimensional planar FEM model was analyzed in the coupled temperature-displacement solver in ABAQUS. The temperature distribution at the end of the load illustrated that built-up heat appeared in the center of the structure. The maximal temperature is in agreement with the one calculated by the empirical formula. With the increase of the temperature caused by inelastic dissipation comes a reduction in the dissipated energy and dynamic stiffness. Since viscoelastic materials exhibit better dissipation behavior when subjected to shear load, in the future research the analysis will be implemented in more styles of load such as bend, compression and hybrid condition. Besides, the IHF coefficient is a key factor for determining the dissipated energy due to the inelastic deform. The value of the IHF will be evaluated precisely by an experiment in the next step.

Acknowledgments: The work was funded by the National Natural Science Foundation for Young Scientists of China (Grant No. 51405323), the National Natural Science Foundation for Young Scientists of China (Grant No. 51305288).

Author Contributions: Jun Wang put forward to the method and contributed the manuscript. Dagang Sun gave some writing and theory suggestion. Shizhong Liu helped simulate coupled solution. Xin Zhang provided some program for post process.

Conflicts of Interest: The authors declare no conflict of interest.

References

1. Ward, I.M.; Sweeney, J. Chapter 2 The mechanical properties of polymers: General considerations. In *Mechanical Properties of Solid Polymers*, 2nd ed.; Wiley: Hoboken, NJ, USA, 2013.
2. Christensen, R. Chapter 3 Thermoviscoelasticity. In *Theory of Viscoelasticity*, 2nd ed.; Academic Press: Waltham, MA, USA, 1982.
3. Ferry, J.D. Chapter 11 Dependence of viscoelastic behavior on temperature and pressure. In *Viscoelastic Properties of Polymers*; Wiley: Hoboken, NJ, USA, 1970.
4. Chang, K.C.; Soong, T.T.; Oh, S.; Lai, M.L. Effect of Ambient Temperature on Viscoelastically Damped Structure. *J. Struct. Eng.* **1992**, *118*, 1955–1973. [[CrossRef](#)]
5. Fang, Q.H.; Zhang, F.P.; Huang, B.Z. Study on Extension Characteristics of Vulcanized Rubber at Different Temperatures. *J. Build. Mater.* **2005**, *8*, 383–386. [[CrossRef](#)]
6. Liu, D.H.; Fan, D.; Ouyang, Y.F.; Wu, C.P. Temperature Effect on Mechanical Properties of Rubber Isolators. *Noise Vib. Control* **2014**, *3*, 203–206. [[CrossRef](#)]
7. Boukamel, A.; Méo, S.; Débordes, O.; Jaeger, M. A Thermo-viscoelastic Model for Elastomeric Behaviour and Its Numerical Application. *Arch. Appl. Mech.* **2001**, *71*, 785–801. [[CrossRef](#)]
8. Rodas, C.O.; Zaïri, F.; Naït-abdelaziz, M. A Finite Strain Thermo-viscoelastic Constitutive Model to Describe the Self-heating in Elastomeric Materials during Low-cycle Fatigue. *J. Mech. Phys. Solids* **2013**, *64*, 396–410. [[CrossRef](#)]
9. Stefanie, R. A Micromechanically Motivated Material Model for the Thermo-viscoelastic Material Behaviour of Rubber-like Polymers. *Int. J. Plast.* **2003**, *19*, 909–940. [[CrossRef](#)]
10. Holzapfel, G.A.; Simo, J.C. A New Viscoelastic Constitutive Model for Continuous Media at Finite Thermomechanical Changes. *Int. J. Solids Struct.* **1996**, *33*, 3019–3034. [[CrossRef](#)]
11. Habibi, M.K.; Tam, L.H.; Lau, D.; Yang, L. Viscoelastic Damping Behavior of Structural Bamboo Material and Its Microstructural Origins. *Mech. Mater.* **2016**, *97*, 184–198. [[CrossRef](#)]
12. Jones, D.I.G. *Handbook of Viscoelastic Vibration Damping*, 1st ed.; Wiley: Hoboken, NJ, USA, 2001.
13. Johnson, A.R.; Chen, T.K. Approximating Thermo-viscoelastic Heating of Largely Strained Solid Rubber Components. *Comput. Methods Appl. Mech. Engrg.* **2005**, *194*, 313–325. [[CrossRef](#)]
14. Shah, S.; Muliana, A.; Rajagopal, K.R. Coupled Heat Conduction and Deformation in a viscoelastic Composite Cylinder. *Mech. Time-Depend. Mater.* **2009**, *13*, 121–147. [[CrossRef](#)]

15. Pešek, L.; Půst, L.; Šulc, P. FEM Modeling of Thermo-Mechanical Interaction in Pre-pressed Rubber Block. *Eng. Mech.* **2007**, *14*, 3–11. Available online: http://www.im.fme.vutbr.cz/pdf/14_1_003.pdf (accessed on 13 March 2017).
16. Banic, M.S.; Stamenkovic, D.S.; Miltenovic, V.D.; Milosevi, M.S.; Miltenovi, A.V.; Djeki, P.S.; Rackov, M.J. Prediction of Heat Generation in Rubber or Rubber-metal Springs. *Therm. Sci.* **2012**, *16*, 527–539. [[CrossRef](#)]
17. Luo, R.K.; Wu, W.X. A Method to Predict the Heat Generation in a Rubber Spring Used in the Railway Industry. *Proc. Inst. Mech. Eng. Part F. J. Rail Rapid Transit* **2005**, *219*, 239–244. [[CrossRef](#)]
18. Khan, A.M. Fully Coupled Heat Conduction and Deformation Analyses of Nonlinear Viscoelastic Composites. *Mech. Time Depend. Mater.* **2012**, *16*, 461–489. [[CrossRef](#)]
19. Lin, Y.J.; Hwang, S.J. Temperature Prediction of Rolling Tires by Computer Simulation. *Math. Comput. Simul.* **2004**, *67*, 235–249. [[CrossRef](#)]
20. Fenza, A.D.; Monaco, E.; Amoroso, F.; Lecce, L. Experimental Approach in Studying Temperature Effects on Composite Material Structures Realized with Viscoelastic Damping Treatments. *J. Vib. Control* **2014**, *22*, 358–370. [[CrossRef](#)]
21. Kerchman, V.; Cheng, S. Experimental Study and Finite Element Simulation of Heat Build-up in Rubber Compounds with Application to Fracture. *Rubber Chem. Technol.* **2003**, *76*, 386–405. [[CrossRef](#)]
22. Zghal, S.; Bouazizi, M.L.; Bouhaddi, N.; Nasri, R. Model Reduction Methods for Viscoelastic Sandwich Structures in Frequency and Time Domains. *Finite Elements Anal. Des.* **2015**, *93*, 12–29. [[CrossRef](#)]
23. Failla, G. An Exact Generalised Function Approach to Frequency Response Analysis of Beams and Plane Frames with the Inclusion of Viscoelastic Damping. *J. Sound Vib.* **2016**, *360*, 171–202. [[CrossRef](#)]
24. Johnson, A.R.; Quigley, C.J.; Mead, J.L. Large Strain Viscoelastic Constitutive Models for Rubber, Part I: Formulations. *Rubber Chem. Technol.* **1994**, *67*, 904–917. [[CrossRef](#)]
25. Quigley, C.J.; Mead, J.; Johnson, A.R. Large Strain Viscoelastic Constitutive Models for Rubber, Part II: Determination of Material Constants. *Rubber Chem. Technol.* **1995**, *68*, 230–247. [[CrossRef](#)]
26. Systèmes, D. ABAQUS 6.14. Available online: <http://abaqus.software.polimi.it/v6.14/index.html> (accessed on 10 March 2017).
27. Ghazaly, N.M. ABAQUS Analysis User's Manual, Vol 2-abaqus 6.10.
28. Holzapfel, G.A.; Reiter, G. Fully Coupled Thermomechanical Behaviour of Viscoelastic Solids Treated with Finite Elements. *Int. J. Eng. Sci.* **1995**, *33*, 1037–1058. [[CrossRef](#)]
29. Rittel, D. On the Conversion of Plastic Work to Heat during High Strain Rate Deformation of Glassy Polymers. *Mech. Mater.* **1999**, *31*, 131–139. [[CrossRef](#)]
30. Gent, A.N.; Hertz, D.L.; Hamed, G.R. Chapter 4 Dynamic mechanical properties. In *Engineering with Rubber—How to Design Rubber Components*, 2nd ed.; Hanser Gardner Publications, Carl Hanser Publishers: Cincinnati, OH, USA, 2001.
31. GB/T 15168-2013. Vibration and shock isolators measuring method for its static and dynamic characteristics. Available online: http://www.sac.gov.cn/was5/web/search?channelid=97779&templet=gjcxjg_detail.jsp&searchword=STANDARD_CODE='GB/T15168-2013'&XZ=T&STANDARD_CODE=GB/T15168-2013 (accessed on 10 March 2017).

